Applied Physics Express 6 (2013) 062102
http://dx.doi.org/10.7567/APEX.6.062102

Green Semipolar ($20\bar{2}\bar{1}$) InGaN Light-Emitting Diodes with Small Wavelength Shift and Narrow Spectral Linewidth

Yuji Zhao[1*], Sang Ho Oh[2], Feng Wu[1], Yoshinobu Kawaguchi[1], Shinichi Tanaka[1], Kenji Fujito[3], James S. Speck[1], Steven P. DenBaars[1,2], and Shuji Nakamura[1,2]

[1]*Materials Department, University of California, Santa Barbara, CA 93106, U.S.A.*
[2]*Electrical and Computer Engineering Department, University of California, Santa Barbara, CA 93106, U.S.A.*
[3]*Optoelectronic Laboratory, Mitsubishi Chemical Corporation, Ushiku, Ibaraki 300-1295, Japan*
E-mail: yujizhao@engineering.ucsb.edu

Received February 7, 2013; accepted May 8, 2013; published online May 24, 2013

We study the optical spectral properties for green semipolar ($20\bar{2}\bar{1}$) and ($20\bar{2}1$) light-emitting diode (LED) with same indium compositions. Compared to ($20\bar{2}1$) devices, the fabricated ($20\bar{2}\bar{1}$) micro-LED (~0.005 mm^2) showed negligible blue shift and smaller full width at half maximum (FWHM) up to extremely high current densities (10,000 A/cm^2). Theoretical simulation indicates that the ($20\bar{2}\bar{1}$) InGaN quantum well (QW) has reduced polarization-related effects due to combined effects of electric field cancelling and Coulomb screening effect. In addition, the packaged device performance for small-area (~0.144 mm^2) semipolar green ($20\bar{2}\bar{1}$) and ($20\bar{2}1$) LEDs were also discussed. The green ($20\bar{2}\bar{1}$) LED showed smaller wavelength shift and narrower FWHM than green LEDs fabricated on other planes.

III–nitride semiconductors and their alloys possess direct band gaps throughout the entire visible spectral region, which make them ideal materials for the fabrication of light-emitting diodes (LEDs) and laser diodes (LDs).[1)] To date, violet and blue LEDs based on *c*-plane GaN crystals have already been successfully commercialized for a wide range of applications, including traffic signals, backlighting sources for liquid-crystal display, and general lighting. For these commercial "polar" *c*-plane devices, one problem that has persisted since their early demonstration in the 1990s and is becoming increasingly troublesome is the large polarization fields inside their active region, which separate the electron and hole wave functions in the quantum wells (QWs) and reduce the radiative recombination rate.[2,3)] This polarization-related effect, combined with reduced active region material quality, is exacerbated for QWs with higher indium compositions, which is therefore considered as one of the major reasons for the efficiency loss of nitride optoelectronic devices operating at longer wavelength (i.e., $>$ 500 nm), a phenomenon known as the "green gap".[1)] An important sign for this notorious polarization effect is the large electroluminescence (EL) wavelength shift with increasing current injection, which is widely observed for commercial *c*-plane devices.[4,5)]

To circumvent this problem, devices grown on nonpolar or semipolar orientations have been proposed to eliminate or reduce the polarization fields,[6,7)] and were theoretically predicted to have higher radiative recombination rates than *c*-plane devices.[8)] Among various semipolar/nonpolar planes, the ($20\bar{2}1$) plane has attracted significant attention due to the demonstration of high-performance green LDs and LEDs.[9,10)] However, the observed wavelength shift is still relatively large on these devices.[10)] More recently, violet[11)] and blue[12)] LEDs fabricated on the semipolar ($20\bar{2}\bar{1}$) plane showed promising performance with high efficiency and low droop at high current densities. Several other advantages including increased optical polarization ratio[13)] and high indium incorporations[14)] were also reported for green ($20\bar{2}\bar{1}$) devices. In this work, we report a green InGaN/GaN LED on a free-standing semipolar ($20\bar{2}\bar{1}$) bulk GaN substrate with extremely small wavelength shift and narrow spectral linewidth. Device simulations show that semipolar ($20\bar{2}\bar{1}$) QWs have reduced polarization effect. Experimental results on device efficiency and light output power of green ($20\bar{2}\bar{1}$) LED are also presented.

LED epitaxial layers were grown by conventional metal organic chemical vapor deposition (MOCVD) on free-standing semipolar GaN substrates supplied by Mitsubishi Chemical Corporation. The device structure consisted of a 1 μm Si-doped n-type GaN layer, a 3 nm InGaN single-quantum-well (SQW) active region, a Mg-doped 16 nm $Al_{0.15}Ga_{0.85}N$ electron-blocking layer (EBL), and a 60 nm p-type GaN layer. For comparison, identical SQW LED structures were prepared on both semipolar ($20\bar{2}\bar{1}$) and ($20\bar{2}1$) substrates. A higher growth temperature ($\Delta T \sim$ 30 K) was used for ($20\bar{2}\bar{1}$) SQW to achieve similar indium compositions on the two planes.[14)] The indium compositions of the samples were confirmed by the photoluminescence (PL) measurement and X-ray diffraction (XRD) analysis. According to our studies, for LEDs emitting at 500 nm, the indium compositions of ($20\bar{2}1$) and ($20\bar{2}\bar{1}$) QWs were estimated to be 30 and 32% respectively, with an error bar of ±3%. The detailed study for the indium measurement will be published in another paper. To study the spectral characteristics, micro-LEDs of 80 μm diameter were fabricated on both ($20\bar{2}\bar{1}$) and ($20\bar{2}1$) samples and both samples were characterized by room-temperature EL measurement under pulsed conditions (1% duty cycles).

Figure 1 demonstrates the (a) EL peak wavelength and (b) full width at half maximum (FWHM) for the green semipolar ($20\bar{2}1$) and ($20\bar{2}\bar{1}$) SQW micro-LEDs at various current densities. While most of the InGaN LEDs[4,5,10,15)] are characterized by a large wavelength shift due to polarization-related electric fields, the ($20\bar{2}\bar{1}$) LED showed a negligible wavelength shift up to extremely high current densities (10,000 A/cm^2). Conversely, a 15 nm wavelength shift was observed for ($20\bar{2}1$) devices at the same current density range. Furthermore, the ($20\bar{2}\bar{1}$) LED exhibited a much narrower linewidth than the ($20\bar{2}1$) LED. At 1,000 and 10,000 A/cm^2, the FWHMs for ($20\bar{2}\bar{1}$) LED were 26.2 and 33.4 nm, respectively, which are significantly smaller than the values for ($20\bar{2}1$) LED (30.4 and 40.5 nm). The narrow spectral linewidth is especially desirable for LDs; thus, it may be advantageous to fabricate LDs on the ($20\bar{2}\bar{1}$) plane.

The small wavelength shift and narrow FWHM for the ($20\bar{2}\bar{1}$) green LED are consistent with previously reported

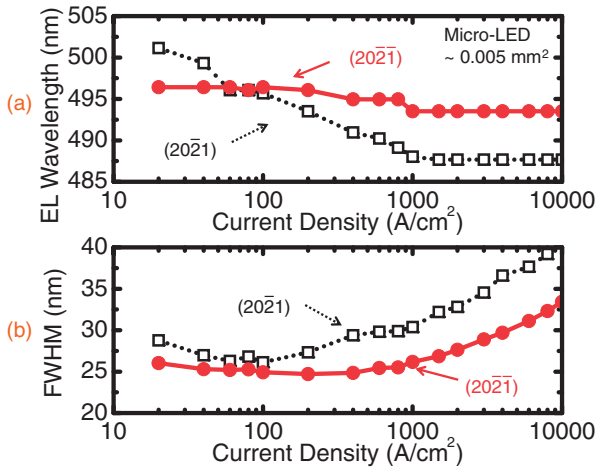

Fig. 1. (a) EL peak wavelength and (b) FWHM curves as functions of current density for green semipolar (20$\bar{2}$1) and (20$\bar{2}\bar{1}$) SQW micro-LEDs under pulsed operation.

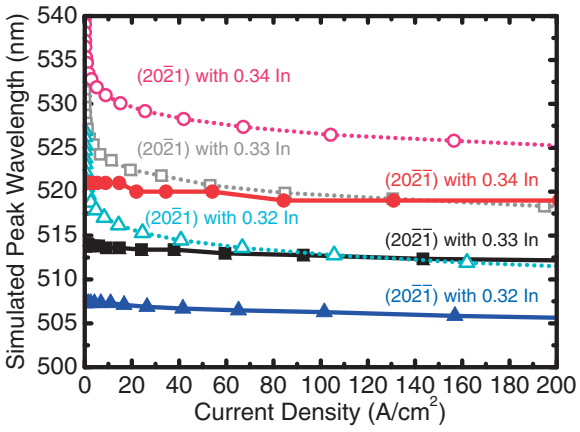

Fig. 2. Simulated peak emission wavelength curves as a function of current density for green semipolar (20$\bar{2}\bar{1}$) (solid lines) and (20$\bar{2}$1) (dashed lines) SQW green LEDs with indium compositions of 0.32, 0.33, and 0.34.

(20$\bar{2}\bar{1}$) violet-blue and blue LEDs,[11,12] which are likely related to the flat QW potential profile that resulted from the cancellation of the p–n junction built-in (E_{bi}) and the polarization-related (E_{pz}) electric field. In our previous study, we showed that appropriate combinations of the two fields will lead to a relatively flat potential profile and nearly completely eliminates the blue shift with increasing injection current densities.[14] Figure 2 shows the simulated peak emission wavelengths as a function of current density for semipolar (20$\bar{2}\bar{1}$) and (20$\bar{2}$1) SQW LEDs with various indium compositions, using the commercial SiLENSe package developed by the STR Group.[16] For the simulation, a one-dimensional (1D) Schrödinger–Poisson equation containing a drift-diffusion model was solved self consistently, where effects of strain and polarization for arbitrary orientations were also included. The strain and piezoelectric charges for nonpolar and semipolar heterostructures were calculated via the approach in Ref. 17, where the piezoelectric and spontaneous polarization constants were taken from Refs. 18–21. At any given indium composition, the simulated (20$\bar{2}\bar{1}$) LEDs showed a stable emission wavelength with increasing current density, while a large blue shift ($\Delta\lambda \sim 10$ to 15 nm) was found for (20$\bar{2}$1) LEDs. The simulated results were consistent with previous EL measurements on micro-LEDs, which are explained by the cancelling of electric field inside quantum well. For (20$\bar{2}$1) QW, E_{bi} is parallel to E_{pz} and is additive to E_{pz}. For (20$\bar{2}\bar{1}$) QW, E_{bi} is antiparallel to E_{pz} with a similar magnitude, which nearly cancels each other. As a result, the (20$\bar{2}\bar{1}$) QW will have a flatter potential profile while the (20$\bar{2}$1) QW will have a triangular shaped profile. In addition, we also considered the Coulomb screening of the polarization-related electric field due to the carrier injection. Our simulation showed a higher carrier concentration on the (20$\bar{2}$1) plane than that on the (20$\bar{2}\bar{1}$) plane. For example, at 10 A/cm^2, the electron carrier concentrations in (20$\bar{2}$1) and (20$\bar{2}\bar{1}$) LEDs were 3.6×10^{19} and 7.3×10^{18} cm^{-3}, respectively. This will lead to a more prominent change to the triangular shaped (20$\bar{2}$1) QW (QW profile tends to flatten and the effective band gap increases) than the flat (20$\bar{2}\bar{1}$) QW, which will result in a larger wavelength shift with increasing current density on (20$\bar{2}$1) LEDs. Conversely, the (20$\bar{2}\bar{1}$) devices show very little wavelength shift.

However, a major drawback for the stable emission on (20$\bar{2}\bar{1}$) devices is a shorter QW emission wavelength for a given indium composition compared to (20$\bar{2}$1) devices. At low current densities, the simulated (20$\bar{2}$1) LEDs show a longer emission wavelength ($\lambda \sim 540$ nm) than that on (20$\bar{2}\bar{1}$) LEDs ($\lambda \sim 520$ nm) at the same indium composition (In $\sim$ 0.34). When the current density increases, the wavelength benefit on (20$\bar{2}$1) LEDs is greatly offset by the large blue shift due to the polarization-related effect, while the wavelength of (20$\bar{2}\bar{1}$) LEDs remains nearly constant. The wavelength difference between two LEDs is reduced to around 5 nm at a current density of 200 A/cm^2. This simulated result is consistent with experimental findings and theoretical predictions. However, the simulation still suggests that a higher indium composition (In $\sim$ 0.34) is required for (20$\bar{2}\bar{1}$) LEDs to achieve the same wavelength ($\lambda \sim 520$ nm) than that for (20$\bar{2}$1) LEDs (In $\sim$ 0.33), even at high current densities. This may lead to extra material challenge for the (20$\bar{2}\bar{1}$) plane to achieve high-performance long-wavelength devices.

Figure 3 presents the simulated normalized spectral for (a) (20$\bar{2}\bar{1}$) and (b) (20$\bar{2}$1) InGaN SQW green LEDs with 0.33 indium composition at various current densities. The simulated (20$\bar{2}\bar{1}$) LEDs showed a much more stable peak wavelength than the (20$\bar{2}\bar{1}$) LEDs, which is consistent with previous simulation. Furthermore, the (20$\bar{2}\bar{1}$) LEDs also showed narrower spectral linewidth. Table I summarizes the FWHMs at various current densities for the simulated spectral of (20$\bar{2}\bar{1}$) and (20$\bar{2}$1) SQW green LEDs. The smaller FWHM on (20$\bar{2}\bar{1}$) LEDs is consistent with experimental results, which is possibly due to the reduced polarization-related effect. The simulation did not consider the difference in material quality, such as different indium compositional fluctuations between the two planes, which may also affect the spectral properties of InGaN optoelectronic devices.[22] Due to increased indium incorporation, a higher temperature is often required for (20$\bar{2}\bar{1}$) InGaN QW growth compared to (20$\bar{2}$1) QW, which may lead to high quality (20$\bar{2}\bar{1}$) InGaN layer with less compositional fluctuations.[14] This will reduce the potential fluctuations and associated localized

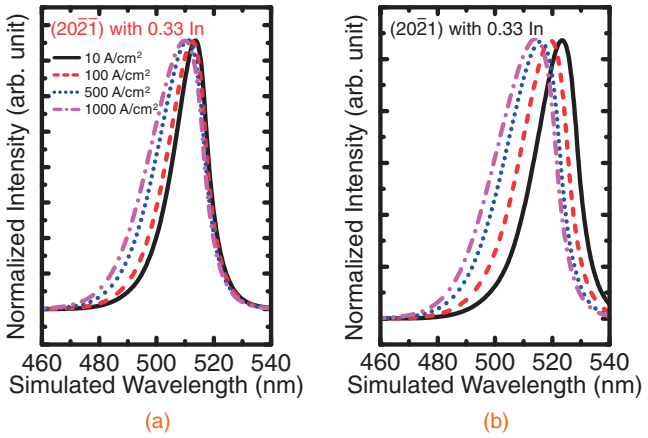

Fig. 3. Simulated spectral for (a) (20$\bar{2}\bar{1}$) and (b) (20$\bar{2}$1) SQW green LEDs with an indium composition of 0.33 at various current densities.

Table I. Simulated FWHMs (nm) at various current densities for semipolar (20$\bar{2}\bar{1}$) and (20$\bar{2}$1) green SQW LEDs with an indium composition of 0.33.

	Current density (A/cm^2)			
	10	100	500	1000
(20$\bar{2}\bar{1}$)	13	15	18	21
(20$\bar{2}$1)	17	19	22	24

states, which will in return contribute to improved spectral properties of (20$\bar{2}\bar{1}$) devices.[23,24] A more thorough study, including comprehensive material characterizations, is currently underway to fully understand this problem.

Finally, we fabricated a green LED on semipolar (20$\bar{2}\bar{1}$) GaN substrate. The LED has the same SQW structure as the previous samples. For the LED fabrication, a rectangular mesa pattern ($490 \times 292\,\mu m^2$) was formed by conventional lithography and chlorine-based inductively coupled plasma (ICP) etching after an indium tin oxide (ITO) current-spreading layer was deposited by electron beam evaporation. Ti/Al/Ni/Au n-type contacts and Ti/Au pads were deposited on the topside of the device by electron beam evaporation and a conventional lift-off process. The backside of the LED was roughened[25] and packaged on silver headers with silicon truncated-cone encapsulants. Room-temperature EL measurements under pulsed conditions with a duty cycle of 1% were performed in a calibrated integrating sphere.

Figure 4 presents light output power and external quantum efficiency (EQE) as functions of drive current for the fabricated green (20$\bar{2}\bar{1}$) SQW LED (chip area ~ 0.144 mm^2), where the optical image of this LED is presented as inset. The experimental results of a (20$\bar{2}$1) green LED with identical structure are also plotted as reference. At a forward current of 20 mA, the semipolar (20$\bar{2}\bar{1}$) LED had an output power of 5.8 mW and an EQE of 11.9%, which is lower but comparable to that of the (20$\bar{2}$1) green LEDs. Due to the higher indium compositions that required for green emission, semipolar (20$\bar{2}\bar{1}$) long wavelength devices ($\lambda > 500$ nm) are naturally more prone to various defects.[26] This may explain the reduced performance for (20$\bar{2}\bar{1}$) green LEDs compared to (20$\bar{2}$1) devices. In addition, the green (20$\bar{2}\bar{1}$) LED shows a large efficiency droop compared with violet-blue and blue (20$\bar{2}\bar{1}$) LEDs.[11,12] To further improve the

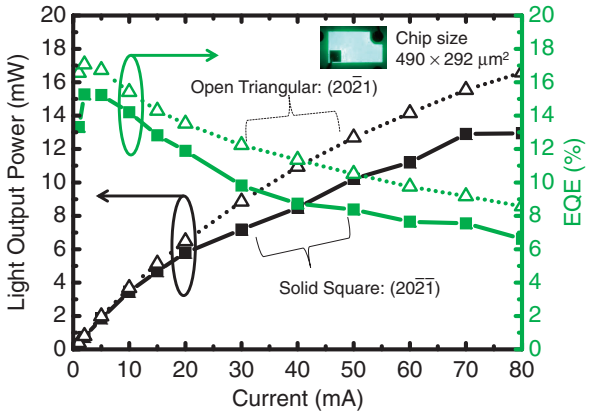

Fig. 4. Light output power and external quantum efficiency (EQE) curves as functions of drive current for a packaged green semipolar (20$\bar{2}\bar{1}$) SQW LED (solid square) under pulsed operation. The results for a packaged green semipolar (20$\bar{2}$1) SQW LED (open triangular) with identical structure are also plotted as reference.

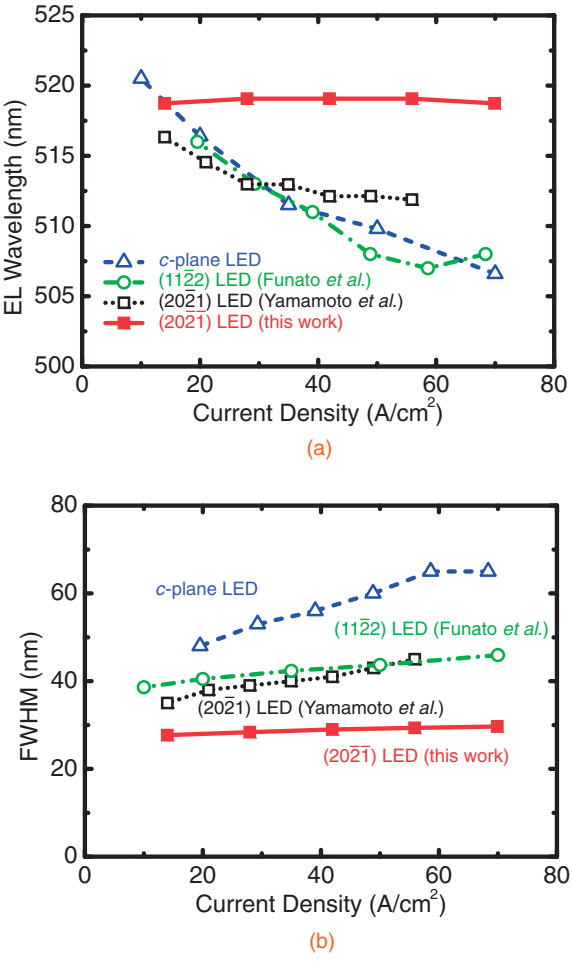

Fig. 5. (a) EL peak wavelength and (b) FWHM curves as functions of current density for the green (20$\bar{2}\bar{1}$) SQW LED.

device performance, green (20$\bar{2}\bar{1}$) LEDs with a thicker QW structure or multiple-quantum-well (MQW) structure will be utilized to reduce the droop ratio.

Figure 5 shows the (a) EL peak wavelength and (b) FWHM for the (20$\bar{2}\bar{1}$) SQW green LEDs at various current densities. For comparison, previously reported results for SQW green LEDs on (20$\bar{2}$1) and (11$\bar{2}\bar{2}$) planes[10,24] and

experimental results on *c*-plane SQW green LEDs are also plotted as reference. While all the other LEDs show a 10 to 15 nm wavelength shift with increasing current density, the $(20\bar{2}\bar{1})$ LED exhibits almost no wavelength shift for the same current density range, which is consistent with previous micro-LED results. In addition, the $(20\bar{2}\bar{1})$ LED also shows the smallest FWHM compared with the reference devices. To the best of the authors' knowledge, such small wavelength shift and narrow spectral linewidth have never been reported for green InGaN LEDs.

In summary, we have demonstrated green $(20\bar{2}\bar{1})$ LEDs with extremely small wavelength shift and narrow spectral linewidth. Theoretical simulation indicates that $(20\bar{2}\bar{1})$ InGaN QWs have reduced polarization-related effects. These results suggest that specific semipolar orientations may provide benefits for stable-emission LEDs and LDs for display and lighting applications.

Acknowledgments The authors acknowledge the support of the Solid State Lighting and Energy Center at UCSB. A portion of this work was done at the UCSB nanofabrication facility, part of the National Science Foundation (NSF)-funded National Nanotechnology Infrastructure Network (NNIN).

1) S. Nakamura: MRS Bull. **34** (2009) 101.
2) P. Waltereit, O. Brandt, A. Trampert, H. T. Grahn, J. Menniger, M. Ramsteiner, M. Reiche, and K. H. Ploog: Nature (London) **406** (2000) 865.
3) F. Bernardini and V. Fiorentini: Phys. Status Solidi B **216** (1999) 391.
4) S. Nakamura, T. Mukai, and M. Senoh: J. Appl. Phys. **76** (1994) 8189.
5) C. Wetzel, T. Salagaj, T. Detchprohm, P. Li, and J. S. Nelson: Appl. Phys. Lett. **85** (2004) 866.
6) M. C. Schmidt, K. C. Kim, H. Sato, N. Fellows, H. Masui, S. Nakamura, S. P. DenBaars, and J. S. Speck: Jpn. J. Appl. Phys. **46** (2007) L126.
7) Y. Zhao, J. Sonoda, I. Koslow, C. C. Pan, H. Ohta, J. S. Ha, S. P. DenBaars, and S. Nakamura: Jpn. J. Appl. Phys. **49** (2010) 070206.
8) S. H. Park and D. Ahn: Appl. Phys. Lett. **90** (2007) 013505.
9) Y. Enya, Y. Yoshizumi, T. Kyono, K. Akita, M. Ueno, M. Adachi, T. Sumitomo, S. Tokuyama, T. Ikegami, K. Katayama, and T. Nakamura: Appl. Phys. Express **2** (2009) 082101.
10) S. Yamamoto, Y. Zhao, C. C. Pan, R. B. Chung, K. Fujito, J. Sonoda, S. P. Denbaars, and S. Nakamura: Appl. Phys. Express **3** (2010) 122102.
11) Y. Zhao, S. Tanaka, C. C. Pan, D. Feezell, K. Fujito, J. S. Speck, S. P. DenBaars, and S. Nakamura: Appl. Phys. Express **4** (2011) 082104.
12) C. C. Pan, S. Tanaka, F. Wu, Y. Zhao, J. S. Speck, S. Nakamura, S. P. DenBaars, and D. Feezell: Appl. Phys. Express **5** (2012) 062103.
13) Y. Zhao, S. Tanaka, Q. Yan, C. Y. Huang, R. B. Chung, C. C. Pan, K. Fujito, D. Feezell, C. G. Van de Walle, J. S. Speck, S. P. DenBaars, and S. Nakamura: Appl. Phys. Lett. **99** (2011) 051109.
14) Y. Zhao, Q. Yan, C. Y. Huang, S. C. Huang, P. S. Hsu, S. Tanaka, C. C. Pan, Y. Kawaguchi, K. Fujito, C. G. Van de Walle, J. S. Speck, S. P. DenBaars, S. Nakamura, and D. Feezell: Appl. Phys. Lett. **100** (2012) 201108.
15) H. Sato, A. Tyagi, H. Zhong, N. Fellows, R. B. Chung, M. Saito, K. Fujito, J. S. Speck, S. P. DenBaars, and S. Nakamura: Phys. Status Solidi: Rapid Res. Lett. **1** (2007) 162.
16) V. F. Mymrin, K. A. Bulashevich, N. I. Podolskaya, I. A. Zhmakin, S. Yu. Karpov, and Yu. N. Makarov: Phys. Status Solidi C **2** (2005) 2928.
17) A. E. Romanov, T. J. Baker, S. Nakamura, and J. S. Speck: J. Appl. Phys. **100** (2006) 023522.
18) J. G. Gualtieri, J. A. Kosinski, and A. Ballato: IEEE Trans. Ultrason. Ferroelectr. Freq. Control **41** (1994) 53.
19) A. E. Romanov, P. Waltereit, and J. S. Speck: J. Appl. Phys. **97** (2005) 043708.
20) S. Nakamura, S. Pearton, and G. Fasol: *The Blue Laser Diode: The Complete Story* (Springer, Berlin, 2000) 2nd ed.
21) F. Bernardini, V. Fiorentini, and D. Vanderbilt: Phys. Rev. B **56** (1997) R10024.
22) Y. R. Wu, R. Shivaraman, K. C. Wang, and J. S. Speck: Appl. Phys. Lett. **101** (2012) 083505.
23) S. F. Chichibu, T. Azuhata, T. Sota, and S. Nakamura: Appl. Phys. Lett. **69** (1996) 4188.
24) M. Funato, M. Ueda, Y. Kawakami, Y. Narukawa, T. Kosugi, M. Takahashi, and T. Mukai: Jpn. J. Appl. Phys. **45** (2006) L659.
25) Y. Zhao, J. Sonoda, C. C. Pan, S. Brinkley, I. Koslow, K. Fujito, H. Ohta, S. P. DenBaars, and S. Nakamura: Appl. Phys. Express **3** (2010) 102101.
26) Y. Zhao, F. Wu, C. Y. Huang, Y. Kawaguchi, S. Tanaka, K. Fujito, J. S. Speck, S. P. DenBaars, and S. Nakamura: Appl. Phys. Lett. **102** (2013) 091905.